Morphophysiological and biochemical responses of *Schedonorus arundinaceus* to Zinc (II) excess: insights from biomarkers and elemental accumulation

Respuestas morfofisiológicas y bioquímicas de *Schedonorus arundinaceus* al exceso de zinc (II): Perspectivas sobre biomarcadores y acumulación elemental

Matias Alberto Gonzalez [1*], Valeria Bernardo [1], Sebastián Garita [1], Josefina Plaza Cazón [2], Cecilia Arango [1], Marcelo Paulo Hernández [3, 4], Marcela Ruscitti [1, 5]

Originales: *Recepción:* 17/11/2023 - *Aceptación:* 04/07/2024

Abstract

Excessive levels of zinc have detrimental effects on plant physiology and morphology, hindering growth and development. This study aimed to elucidate the morphophysiological and biochemical mechanisms of *Schedonorus arundinaceus* in response to high concentrations of zinc exposure and to investigate the correlation between these parameters to identify potential stress biomarkers in this species. Plants were exposed to seven zinc concentrations (0-500-1000-1500-2000-2500-3000 µM) for 50 days. The results showed decreased dry weight, root area, photosynthetic pigments, root soluble proteins and stomatal conductance with increasing zinc concentrations. Conversely, proline, malondialdehyde and leaf-soluble protein content increased. Histological observations revealed altered stomata size and abnormalities in root tissue. Zinc accumulation exceeded phytotoxic thresholds (100-400 mg kg^{-1}) even at lower concentrations, reaching a maximum of 3432 mg kg^{-1} in shoots. Visible Zn-P crystals were observed on leaf surfaces at the highest zinc treatment. These results suggest that *S. arundinaceus* possesses a notable capacity to bioaccumulate zinc, particularly in the roots. Furthermore, the strong correlation between proline levels and zinc biomass concentration suggests its potential use as a stress biomarker for zinc-induced stress in this species.

Keywords
zinc phytotoxicity • stress adaptations • root damage • physiological response

1 Instituto de Fisiología Vegetal (INFIVE-CCT La Plata). Diagonal 113 N° 495 (B1900) La Plata, Buenos Aires. Argentina. *magonzalez921994@gmail.com
2 Centro de Investigación y Desarrollo en Fermentaciones Industriales (CINDEFI-CCT La Plata). Calle 50 N° 227 (B1900) La Plata. Buenos Aires. Argentina.
3 Universidad Nacional de La Plata. Facultad de Ciencias Agrarias y Forestales. Laboratorio de Morfología Comparada de Espermatofitas (LAMCE). Cátedra de Morfología Vegetal. Avenida 60 y 119 (B1900) La Plata. Buenos Aires. Argentina.
4 Universidad Nacional de La Plata. Museo de Ciencias Naturales. División Plantas Vasculares. Paseo del Bosque S/N° (B1900) La Plata. Buenos Aires.
5 Universidad Nacional del Noroeste de la Provincia de Buenos Aires. Departamento de Ciencias Básicas y Experimentales. Roque Sáenz Peña 456 (B6000) Junín. Buenos Aires. Argentina.

Resumen

Los niveles excesivos de zinc afectan negativamente la fisiología y morfología de las plantas, dificultando su crecimiento y desarrollo. Este estudio tuvo como objetivo dilucidar los mecanismos morfofisiológicos y bioquímicos de *Schedonorus arundinaceus* en respuesta a altas concentraciones de zinc y explorar la correlación entre estos parámetros para identificar posibles biomarcadores de estrés. Las plantas fueron expuestas a siete concentraciones de zinc (0-500-1000-1500-2000-2500-3000 µM) durante 50 días. Se observó una disminución del peso seco, área radicular, pigmentos fotosintéticos, proteínas solubles en raíz y conductancia estomática con el incremento de zinc. No obstante, aumentó el contenido de prolina, malondialdehído y proteínas solubles en hojas. Las observaciones histológicas revelaron alteraciones en el tamaño de los estomas y del tejido radicular. La acumulación de zinc superó los umbrales fitotóxicos (100-400 mg kg^{-1}), alcanzando un máximo de 3432 mg kg^{-1} en hojas. Se observaron cristales de Zn-P en la superficie de las hojas en las máximas concentraciones. Estos resultados sugieren que *S. arundinaceus* posee una notable capacidad para bioacumular zinc, particularmente en las raíces. Además, la fuerte correlación observada entre la prolina y la acumulación de zinc sugiere su potencial uso como biomarcador de estrés inducido por el exceso de zinc en esta especie.

Palabras clave
fitotoxicidad por zinc • adaptación al estrés • daño radical • respuestas fisiológicas

Introduction

Recently, heavy metal (HM) contamination has emerged as a pressing environmental issue. These non-biodegradable and toxic substances can accumulate in water bodies, soil, sediments, and the food chain, posing a significant risk to human health (10). The extensive use of mineral fertilizers and pesticides (38), coupled with the release of untreated urban and industrial effluents (55), has contributed to soil and water pollution (2). In Argentina, this environmental concern is particularly important in the "green belts" -peri-urban areas where commercial fresh vegetable production for urban centers is concentrated. The green belts of La Plata, Florencio Varela and Berazategui are especially significant, accounting for 82% of horticultural farms and 81% of cultivated land. These areas are crucial for fresh food production and significantly impact the local economy (32). The land use in the peri-urban area of La Plata is diverse, including residential areas, heavy industry, wastelands, intensive farmland, forests, cattle-raising areas and quarries. With urban planning lagging, this transitional zone faces competition among urbanization, industrialization and horticultural activities, leading to increased pollution and ecosystem degradation (32). Studies on HM contamination, particularly Zn, in these areas are scarce but indicate that Zn can exceed normal or toxic levels due to industrial and motor emissions (7, 13). High concentrations of Zn, Pb, Cr and Cu, often exceeding toxic limits, owe to excessive pesticide and fertilizer use in horticultural peri-urban areas (11, 41). This evidence suggests that intensive agricultural practices and urban-industrial emissions, waste production and disposal could elevate HM levels in these areas, threatening environmental health and food security (21). While certain HMs are essential for plant growth and development, their accumulation at high levels can be phytotoxic (3). Among these, zinc [Zn(II)] plays a crucial role in normal plant development. It activates multiple enzymes, participates in the synthesis and metabolism of important biomolecules and serves as a key component of the transcription factor family known as "zinc fingers", which regulates cell proliferation and differentiation processes (49). However, excessive levels result in structural and functional abnormalities negatively impacting plant performance (46). Symptoms include chlorosis, necrosis, reduced growth due to inhibited cell division and elongation, reduced CO_2 fixation and carbohydrate transport and alterations in cellular membrane permeability (28).

Within the Poaceae family, several species have demonstrated resilience in harsh environments, quickly colonizing contaminated areas (38). *Schedonorus arundinaceus* (=*Festuca arundinacea*), commonly known as tall fescue, is the most widely used temperate perennial grass throughout the Argentina Humid Pampa region (covering most of Buenos

Aires and parts of Santa Fe Cordoba and La Pampa provinces) due to its broad ecological adaptation and naturalization (45). It has been observed to thrive in soils contaminated with various heavy metals (HMs), including Pb, Cd, Cu, Zn, Ni and Cr (1, 39). Our previous studies have shown that this species can grow normally with elevated Zn(II) concentrations, indicating its potential for phytoremediation (23). Investigating the morpho-physiological and biochemical responses of Zn(II) excess on *S. arundinaceus* in this region is crucial, as it could provide an effective solution for mitigating Zn(II) contamination, thereby improving soil quality and ensuring food security in the area. To effectively manage species, it is crucial to investigate not only the uptake rate of HMs but also the underlying mechanisms that regulate stress response (26). Also, establishing correlations between plant absorption kinetics and key physiological and biochemical parameters can provide valuable insights for identifying biomarkers to assess specific plant stress responses (26). The objective of this study was to elucidate the morpho-physiological and biochemical mechanisms of *S. arundinaceus* that are elicited in response to excessive exposure to high Zn(II) concentrations. Furthermore, we aimed to investigate the correlation between these parameters in order to identify potential stress biomarkers for this species. These findings could offer promising insights into the application of *S. arundinaceus* in phytotechnologies such as phytoremediation, biofortification and phytomining.

Materials and methods

Growth conditions and treatments

This experiment was conducted between August and October in a greenhouse located in La Plata City, Buenos Aires, Argentina. *S. arundinaceus* seeds were disinfected with NaClO (10%) for 5 minutes, rinsed with sterile water and placed in plastic plug trays with 72 cells containing a perlite-vermiculite mixture (1:1 v/v). Weekly applications of half-strength Hoagland nutrient solution (25) were provided. After 14 days, the seedlings were transplanted into hydroponic containers filled with a complete Hoagland nutrient solution (pH 6.2 ± 0.5). Following a 15-day acclimatisation period to the hydroponic conditions, increasing concentrations of Zn(II) (provided as $ZnSO_4 7H_2O$) were added to obtain seven treatments: control (1µM of Zn(II) (0.065 mg L^{-1}), equivalent to the Zn(II) concentration in the Hoagland nutrient solution), 500 µM (32.69 mg L^{-1}), 1000 µM (65.38 mg L^{-1}), 1500 µM (98.07 mg L^{-1}), 2000 µM (130.76 mg L^{-1}), 2500 µM (163.45 mg L^{-1}) and 3000 µM (196.14 mg L^{-1}) of Zn(II). These various concentrations were selected based on a previous experiment (22) to screen for responses that might not be discernible at lower concentrations and to determine the maximum tolerance limit for this species. The pH of the solutions was maintained at 6.2 ± 0.5 using 0.1 N NaOH/HCl and aerated using aeration pumps. The solutions were changed every two weeks throughout the experiment. *S. arundinaceus* plants were harvested 50 days after the initial application of the Zn(II) solutions.

Morpho-physiological and biochemical parameters measured

The dry weight (DW) of roots and shoots was determined at harvest by oven-drying at 80°C until constant weight was achieved. Leaf relative water content (LRWC) was calculated based on the measurements of dry weight (DW), fresh weight (FW) and turgid weight (TW) of 1 cm diameter leaf discs (49). Maximum root length (RL) and root area (RA) were calculated using RhizoVision Explorer v2.0.3 (43, 44). Total chlorophyll and carotenoid contents were determined from a 0.5 cm diameter leaf disk; absorbance measurements were taken at 647, 664, and 480 nm (52). Soluble protein content was measured from 0.1 g of fresh leaves and roots; absorbance was read at 595 nm and protein concentration was calculated using a standard curve prepared with different concentrations of bovine serum albumin (BSA) (SiFMa Chemical Co.) (9). Malondialdehyde (MDA) content was measured from 0.2 g of fresh leaves and roots by reaction with thiobarbituric acid (24). Proline content was measured from 0.1 g of fresh leaves and roots; absorbance was read at 520 nm to calculate proline content per unit of fresh weight (4). Absorbance measurements for the aforementioned parameters were determined using a Shimadzu UV-160 spectrophotometer (Kyoto, Japan).

Stomatal density (StD) was calculated through image capture and digitalization using a Gemalux XSZ-H microscope equipped with a Motic camera and Motic Image Plus 2.0 software (15). Stomatal counting was conducted using a Leitz SM lux optical microscope with a clear drawing camera. Adaxial and abaxial stomatal conductance (StC) were determined using a Decagon SC-1 Porometer between 4 p.m. and 6 p.m. on a sunny day, in the middle portion of fully expanded and non-senescent leaves. For histological observations, roots were decolorized with 50% sodium hypochlorite and 5% chloral hydrate. The tissues were stained with an 80% safranin O alcoholic solution and mounted in gelatin-glycerin (14).

Zn(II) tolerance assessment and bioconcentration analysis

Dried root and shoot samples (0.5 g) were ground and digested using a mixture of HNO_3 and H_2SO_4 (4:1 ratio). The absorbance was read using a Shimadzu AA6650F Atomic Absorption Spectrophotometer (Japan) (8). The bioaccumulation factor (BCF), translocation factor (TF) and tolerance index (TI) were calculated using the following equations:

$$\mathbf{BCF = [Zn(II)_{biomass}]/[Zn(II)_{solution}]; TF = [Zn(II)_{shoots}]/[Zn(II)_{roots}]; TI = [(DW)_{treatment}/(DW)_{control}].}$$

Crystalline formations resembling salt crystals were exclusively observed on the leaf surfaces of plants exposed to the highest concentration of Zn(II) (3000 µM). The composition of these crystals was analyzed using energy-dispersive X-ray analysis (EDX) and examined under scanning electron microscopy (SEM).

Experimental design and data analysis

The experimental design was fully randomized, consisting of 7 treatments with 10 replicates per treatment. The following variables were analyzed in all treatments using 10 replicates per treatment: dry weight, LWRC, root length, root area, total chlorophyll and carotenoids, soluble protein, MDA, proline, Zn content, bioaccumulation and translocation factors and tolerance index. The following variables were analyzed only in the control and maximum Zn concentration (3000 µM) using 10 replicates per treatment: stomatal density and conductance and histological observations. The data were analyzed using analysis of variance (ANOVA), and means were compared using the least significant difference (LSD) test at a significance level of 5% ($p<0.05$) (16). Pearson correlations, involving 24 variables, were determined using R version 4.3.1 software. All results were expressed as mean values with corresponding standard deviations.

Results

Morpho-physiological and biochemical parameters

The DW significantly decreased as the concentrations of Zn(II) increased, with shoots and roots experiencing a reduction of 60% and 45% respectively, at the maximum concentration (figure 1a, page XXX). The RA also showed a significant decrease starting from 1000 µM, while the RL exhibited a significant increase at lower concentrations (figure 1b, page XXX) but remained unchanged at higher concentrations, indicating a potential reduction in secondary root formation. The LRWC remained stable, suggesting a relatively consistent water status in response to Zn(II) exposure (table 1, page XXX). Total chlorophyll and carotenoid contents decreased with increasing Zn(II) concentrations, reaching values 80% and 74% lower than the control at the highest concentration (table 1, page XXX). Significant changes were also observed in soluble protein content. Leaves exhibited a slight increase, being 24% higher under 3000 µM compared to the control, while roots showed a decrease of 40% under the same concentration (table 1, page XXX). The levels of MDA increased in leaves under high Zn(II) stress, reaching values three times higher than the control at 3000 µM. In contrast, root MDA levels remained lower and showed no significant differences among treatments (figure 2a, page XXX). Proline showed a significant increase in both leaves and roots under Zn(II) concentrations of 1500 µM and higher, reaching values in shoots that were 162 times higher than the control, while in roots, it was 13 times higher (figure 2b, page XXX). These findings could indicate the activation of stress-related mechanisms in response to Zn(II) excess, as proline is believed to function as a scavenger of reactive oxygen species (ROS) or as an osmolyte, aiding in the defense against oxidative stress.

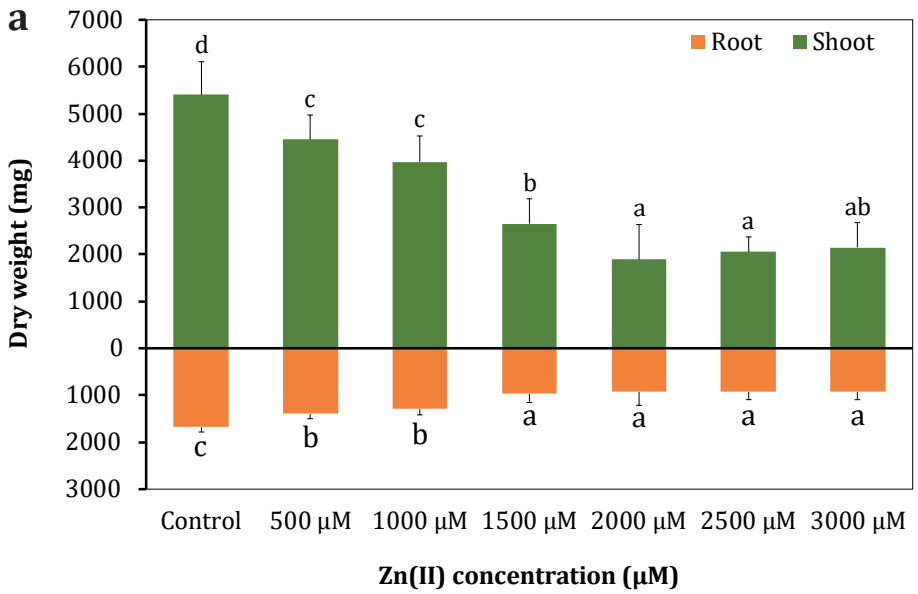

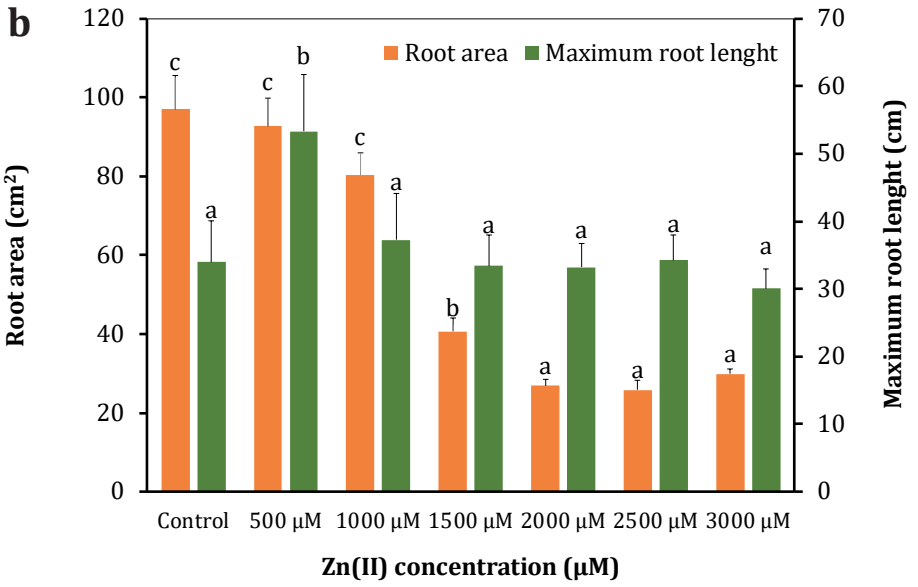

Columns represent mean values of 10 replications, and vertical bars show standard deviation. Columns sharing different letters indicate significant differences ($p < 0.05$).

Las columnas representan los valores medios de 10 repeticiones y las barras verticales muestran la desviación estándar. Las columnas que comparten letras diferentes indican diferencias significativas ($p < 0,05$).

Figure 1. Effect of Zn(II) concentrations on the dry weight (a), root area and maximum root length (b) of *S. arundinaceus*.

Figura 1. Efecto de las concentraciones de Zn(II) sobre el peso seco (a), el área y la longitud radical máxima (b) de *S. arundinaceus*.

Table 1. Effect of Zn(II) concentrations on physiological and biochemical parameters of *S. arundinaceus*.

Tabla 1. Efecto de las concentraciones de Zn(II) sobre los parámetros fisiológicos y bioquímicos de *S. arundinaceus*.

Zn (II) treatment	Leaf water relative content (%)	Total chlorophyll (µg cm^{-2})	Carotenoid (µg cm^{-2})	Shoot proteins (µg mg^{-1} FW)	Root proteins (µg mg^{-1} FW)
Control	80% ± 6% ab	12.88 ± 1.42 d	1.89 ± 0.22 c	5.72 ± 1.5 ab	2.83 ± 0.15 cd
500 µM	80% ± 3% b	10.44 ± 3.13 cd	1.81 ± 0.35 c	4.51 ± 0.63 a	3.19 ± 0.16 d
1000 µM	85% ± 2% b	9.71 ± 2 c	1.32 ± 0.18 c	5.93 ± 1.39 ab	2.71 ± 0.31 c
1500 µM	84% ± 3% b	7.09 ± 1.39 b	1.36 ± 0.15 b	6.13 ± 0.74 bc	2.66 ± 0.15 bc
2000 µM	80% ± 3% ab	6.57 ± 2.04 b	1.06 ± 0.28 b	6.63 ± 0.98 bc	2.26 ± 0.21 b
2500 µM	85% ± 2% b	3.76 ± 0.17 a	0.68 ± 0.04 a	6.51 ± 0.59 bc	1.42 ± 0.2 a
3000 µM	74% ± 2% a	2.58 ± 0.18 a	0.5 ± 0.13 a	7.59 ± 0.72 c	1.68 ± 0.53 a

Data given in the table are means of 10 replications ± standard deviation. For each parameter, data followed by different letters indicate significant differences ($p < 0.05$).

Los datos indicados en la tabla son la media de 10 réplicas ± desviación estándar. Para cada parámetro, los datos seguidos de letras diferentes indican diferencias significativas ($p < 0,05$).

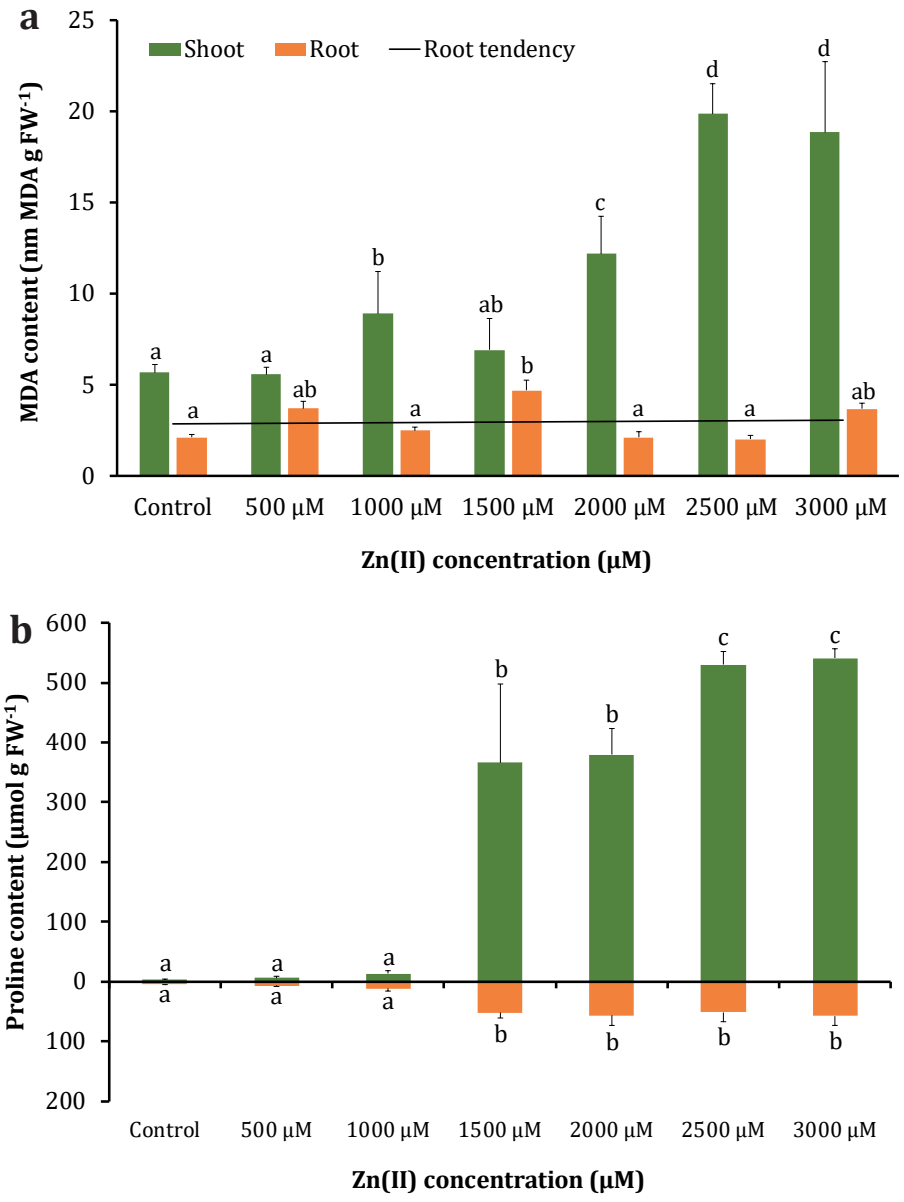

Columns represent mean values of 10 replications, and vertical bars show standard deviation. Columns sharing different letters indicate significant differences ($p < 0.05$).

Las columnas representan los valores medios de 10 repeticiones y las barras verticales muestran la desviación estándar. Las columnas que comparten letras diferentes indican diferencias significativas ($p < 0,05$).

Figure 2. Effect of Zn(II) concentrations on *S. arundinaceus* MDA (a) and proline (b) contents.

Figura 2. Efecto de las concentraciones de Zn(II) en los contenidos de MDA (a) y prolina (b) de *S. arundinaceus*.

Significant differences were observed in adaxial and abaxial stomatal density (StD), conductance (StC), length (StL) and width (StW) exclusively between the control and 3000 µM treatments. Hence, the subsequent results will focus solely on these specific treatments. Both adaxial and abaxial StC decreased, reaching values 2 and 4 times lower than the control under 3000 µM. Adaxial StD was significantly higher, while abaxial StD exhibited the opposite trend. However, total StD did not vary significantly. Although there were no significant differences in adaxial and abaxial StL, a noticeable decrease in abaxial StW was observed (table 2). This suggests that under higher Zn(II) concentrations, smaller and rounder stomata were present. Also, neither non-glandular trichomes nor salt glands were observed on the leaves of plants from all treatments. In terms of root anatomy, the transversal section analysis of control roots revealed a concentric cortical parenchyma composed of orderly to slightly disordered cells, with a vascular cylinder surrounded by endodermis (figure 3a). In contrast, roots exposed to 3000 µM exhibited morphological changes, including protuberances (figure 3b), dorsoventral compression of cortical parenchyma, endodermis and vascular bundles as well as signs of disintegration and medullary proliferation (figure 3c).

Data given in the table are the mean of 10 replications ± standard deviation. For each trait, data followed by different letters indicate significant differences ($p < 0.05$).

Los datos indicados en la tabla son la media de 10 repeticiones ± desviación estándar. Para cada parámetro, los datos seguidos de letras diferentes indican diferencias significativas ($p < 0,05$).

Table 2. Adaxial and abaxial stomatal density (StD), conductance (StC), length (StL), and width (StW) of *S. arundinaceus*.

Tabla 2. Densidad estomática adaxial y abaxial (StD), conductancia (StC), longitud (StL) y latitud (StW) de *S. arundinaceus*.

Zn(II) treatment	Adaxial StC (mmol m^{-2} s^{-1})	Abaxial StC (mmol m^{-2} s^{-1})	Adaxial StD (mm^{-2})	Abaxial StD (mm^{-2})	Adaxial StL (µm)	Adaxial StW (µm)	Abaxial StL (µm)	Abaxial StW (µm)
Control	190 ± 11 b	61 ± 2 a	53 ± 9 a	133 ± 8 b	55 ± 5 a	17 ± 2 a	55 ± 8 a	17 ±1 b
3000 µM	94 ± 24 a	15 ± 4 b	93 ± 8 b	97 ± 7 a	48 ± 4 a	19 ± 2 a	44 ± 7 a	12 ± 2 a

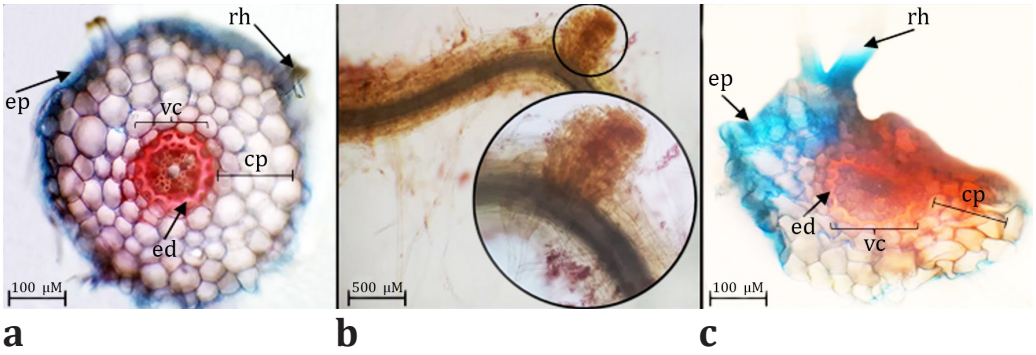

Figure 3. Control roots transversal sections (a), root protuberances observed under 3000 µM (b) and 3000 µM treated roots transversal sections (c) (ep: epidermis, rh: root hair, cp: cortical parenchyma, vc: vascular cylinder, ed: endodermis).

Figura 3. Secciones transversales de las raíces del control (a), protuberancias radiculares observadas bajo 3000 µM (b) y secciones transversales de raíces tratadas con 3000 µM (c) (ep: epidermis, rh: pelo radical, cp: parénquima cortical, vc: cilindro vascular, ed: endodermis).

Zn(II) tolerance assessment and bioaccumulation analysis

S. arundinaceus exhibited significant accumulation of Zn(II), with levels reaching 50 times higher than the control under the 3000 µM treatment, but the highest biomass concentration (7244 mg kg^{-1} DW) was observed under the 2500 µM treatment. Zn(II) distribution showed that roots accumulated more Zn(II) than shoots in the lower

concentrations, but this difference became three times smaller after reaching the 1500 µM concentration (figure 4). BCF values were only higher than 1000 under the 500 µM and 1000 µM treatments, while the TF values remained below 1 in all treatments. The TI exhibited a decrease from 81% to 43% as Zn(II) concentration increased from 500 µM to 3000 µM, respectively (table 3). Crystalline formations resembling salt crystals were exclusively observed on the leaf surfaces of plants exposed to 3000 µM. SEM analysis revealed distinct crystalline structures on the leaf surfaces and EDX analysis confirmed the predominant composition of Zn(II) and P (figure 5, page XXX).

Columns sharing different letters indicate significant differences ($p < 0.05$).

Columns represent mean values of 10 replications, and vertical bars show standard deviation.

Las columnas que comparten letras diferentes indican diferencias significativas ($p < 0,05$).

Las columnas representan los valores medios de 10 repeticiones y las barras verticales muestran la desviación estándar.

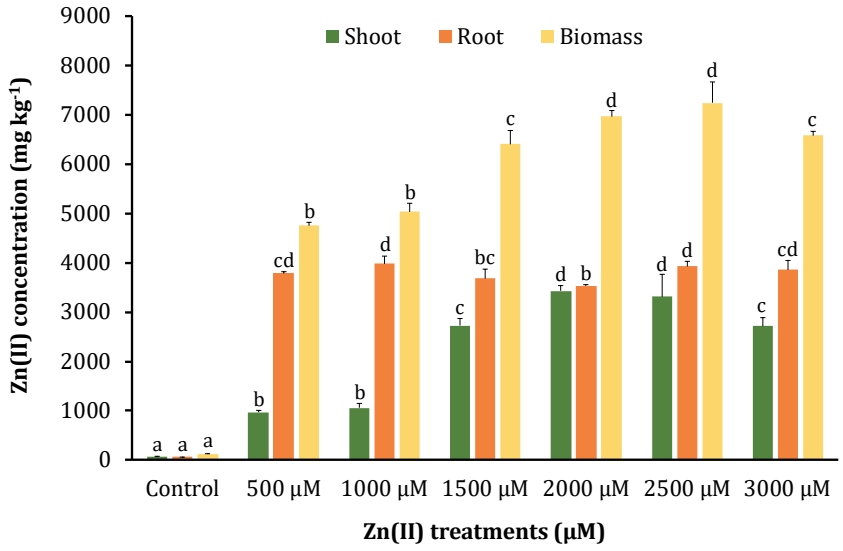

Figure 4. Zn(II) accumulation in shoots, roots, and biomass of *S. arundinaceus*.
Figura 4. Acumulación de Zn(II) en hojas, raíces y biomasa de *S. arundinaceus*.

Table 3. Bioconcentration factor (BCF), translocation factor (TF) and tolerance index (TI).
Tabla 3. Factor de bioconcentración (BCF), factor de translocación (TF) e índice de tolerancia (TI).

Data given in the table are mean of 10 replications ± standard deviation. For each trait, data followed by different letters indicate significant differences ($p < 0.05$).

Los datos que figuran en la tabla son la media de 10 repeticiones ± desviación estándar. Para cada rasgo, los datos seguidos de letras diferentes indican diferencias significativas ($p < 0,05$).

Zn (II) treatment	BCF	TF	TI (%)
Control	247 ± 9 a	0.98 ± 0.09 c	-
500 µM	3650 ± 51 e	0.26 ± 0.01 a	81% ± 14% b
1000 µM	2701 ± 95 d	0.27 ± 0.03 a	73% ± 15% b
1500 µM	415 ± 17 c	0.74 ± 0.04 b	51% ± 12% a
2000 µM	344 ± 5 b	0.97 ± 0.03 c	46% ± 15% a
2500 µM	325 ± 19 b	0.85 ± 0.12 bc	43% ± 15% a
3000 µM	237 ± 3 a	0.71 ± 0.07 b	43% ± 13% a

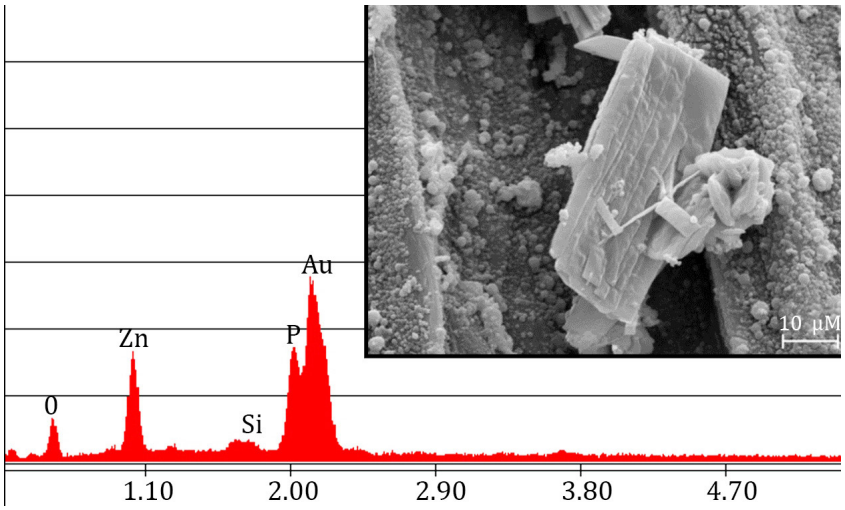

Figure 5. EDX spectra and scanning electron microscopy (SEM) image of the crystals observed on *S. arundinaceus* leaf surfaces exposed to 3000 µM.

Figura 5. Análisis EDX e imagen de microscopía electrónica de barrido (SEM) de los cristales observados en las superficies de las hojas de *S. arundinaceus* expuestas a 3000 µM.

Correlation analysis

Higher correlations were observed between Zn(II) concentrations in leaves and the examined parameters compared to Zn(II) concentrations in roots. The results revealed highly significant positive correlations between shoot Zn(II) content and MDA levels in roots, as well as proline content in shoots and roots. Conversely, shoot and root DW, photosynthetic pigments content, shoot phenolic compounds content and RA exhibited high negative correlations. Root Zn(II) content showed significantly high positive correlations with shoot and root proline content and negative correlations with shoot and root dry weight, shoot phenolics content and RA (figure 6).

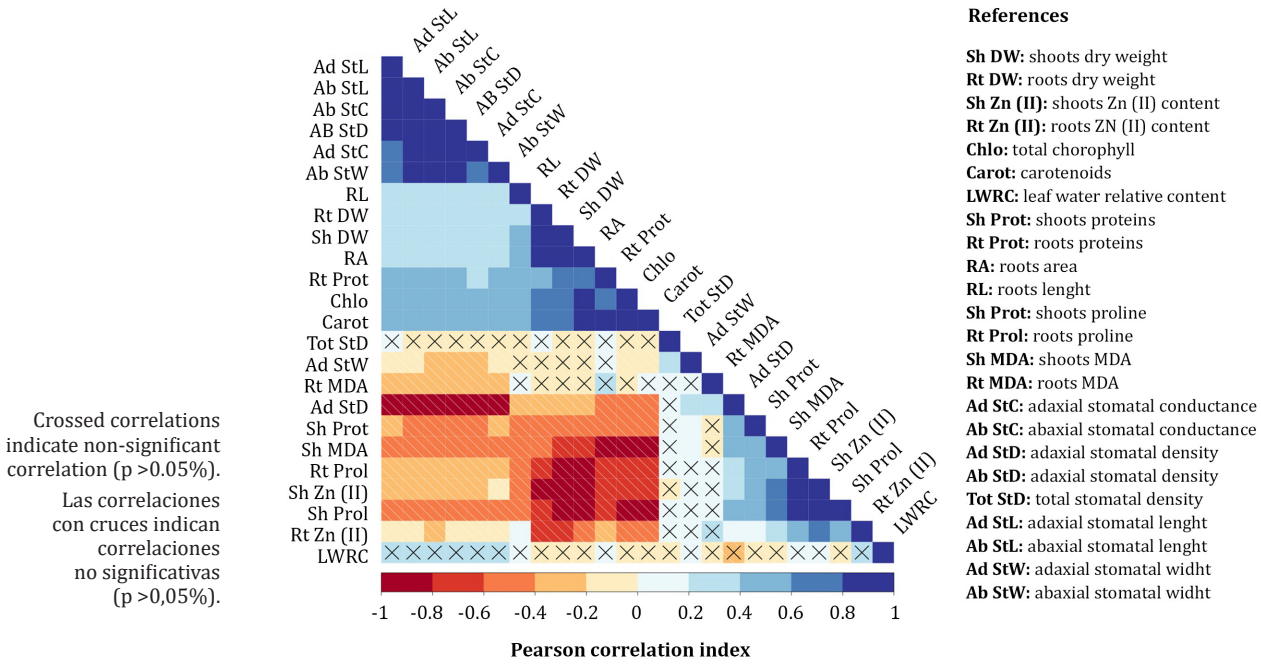

Crossed correlations indicate non-significant correlation (p >0.05%).

Las correlaciones con cruces indican correlaciones no significativas (p >0,05%).

Figure 6. Pearson correlation matrix of various morpho-physiological and biochemical parameters of *S. arundinaceus* exposed to Zn(II) stress.

Figura 6. Matriz de correlación de Pearson de varios parámetros morfofisiológicos y bioquímicos de *S. arundinaceus* expuestos a estrés por Zn(II).

Proline content demonstrated a potential association with a stress threshold bioconcentration of Zn(II) in *S. arundinaceus*. Under the 1500 µM treatment, proline content increased by 27 times in shoots and 5 times in roots compared to the preceding treatment. This significant increase was specific to proline, while other biochemical and physiological parameters displayed gradual changes with increasing Zn(II) concentrations. At 1500 µM, *S. arundinaceus* bioaccumulated 6408 mg kg^{-1} DW, which could be considered a stress threshold limit, as various growth, physiological and biochemical parameters displayed significant alterations beyond this point, indicating a higher stress condition. Furthermore, after this treatment, the shoot concentration of Zn(II) reached similar levels to that of the roots, suggesting that defensive mechanisms were incapable of preventing excessive translocation of Zn(II) to the shoots.

Discussion

S. arundinaceus bioaccumulated high concentrations Zn(II), with a maximum of 7244 ± 424 (SD) mg kg^{-1} DW at 2500 µM Zn(II). Shoot Zn(II) concentrations (970-3432 mg kg^{-1}) exceeded phytotoxic levels, even at lower treatments, as shoot concentrations above 100-400 mg kg^{-1} DW are considered phytotoxic (42). Similar findings were reported in 5-month-old *S. arundinaceus* plants in the vegetative stage, reaching Zn(II) values of 432 and 1099 mg kg^{-1} in shoots and roots, respectively (54). This difference in accumulation observed in comparison to our study could be related to the different substrates (Haplargids soil) or genotypes used in this experiment. Concerning this, other research reported higher concentrations in shoots and roots, reaching up to 6000 and 9000 mg kg^{-1} DW respectively, indicating the presence of a possible ecotype of *S. arundinaceus* and variations in Zn(II) tolerance within the same species (12).

Our study suggests that *S. arundinaceus* acted as an accumulator and phytostabilizer species, exhibiting BCF values exceeding 1000 at lower concentrations but TF values never surpassing 1. After 1500 µM, the distribution pattern of Zn(II) changed significantly, approaching TF values closer to 1. Crystalline formations were observed on the leaves of plants treated with 3000 µM Zn(II), suggesting a potential excretion mechanism. However, it has not been reported that *S. arundinaceus* produce visible Zn(II) crystals through leaf excretion. A study found that *S. arundinaceus* excreted Cd through guttation fluid (18). Some halophyte grasses have salt glands or glandular trichomes, which they use to excrete salts in large quantities, which can also excrete HMs (53). However, *S. arundinaceus* exhibited non-glandular trichomes and lacked salt glands.

We hypothesized that high Zn(II) concentrations caused crystal formation through guttation fluid with Zn-P salts, serving as a tolerance mechanism. This is also correlated with the decrease in shoots Zn(II) content observed between the 2500 µM and 3000 µM treatments. However, further investigation is needed to understand the formation and implications of these Zn-P crystals in Zn(II) tolerance.

Excessive levels of Zn(II) can have negative effects on plant physiology and morphology, including inhibition of cell division and elongation, increased production of ROS and decreased photosynthesis, nutrient uptake and water absorption (28). Our results showed a decrease in general DW, as well as RA reduction with increasing Zn(II) treatments. Moreover, TI values indicated that Zn(II) inhibited growth, reaching values below 60% at 1000 µM and higher concentrations. Higher TI values suggest plant tolerance to HMs without significant growth inhibition (48). Additionally, morphological and anatomical abnormalities, such as small protuberances, were observed in roots treated with 3000 µM Zn(II). It was found that Zn(II)-treated *Brassica napus* root epidermal cells exhibited distortion, smaller size, shrinkage and irregular alignment, which was associated with growth inhibition, reduced nutrient absorption and damage to the root apex (30).

Accumulation of HMs in root cell walls diminishes their elasticity, leading to alterations in water uptake. However, our experiment did not show significant differences in LRWC, suggesting that the observed morphological changes were insufficient to affect root water uptake. Similar findings have been reported for *Psidium guajava* exposed to high Ni levels, where enhanced vacuole volume was proposed as a contributing factor (6). Furthermore, a decrease in stomatal conductance and the presence of smaller stomata were observed at

3000 μM Zn(II), as reported in *Citrus reticulata* (47), suggesting that these alterations may represent an adaptive response aimed at mitigating excessive water loss. Zn(II) excess leads to a deficiency in carbonic anhydrase, which affects HCO_3^- concentration in the guard cells and K^+ uptake, consequently resulting in alterations in guard cell morphology and stomatal shape (37). *S. arundinaceus* exhibited a reduction in photosynthetic pigments content. Similar results were reported in other plant species exposed to high Zn(II) concentrations (33). This decrease can be attributed to the inhibition of chlorophyll synthesis caused by Zn(II)-induced deficiencies of Mg(II) and Fe(II) (29).

Excessive Zn(II) bioaccumulation triggers ROS overproduction, leading to oxidative stress and membrane damage (51). Our study revealed an increase in shoot MDA levels, while root levels did not show significant differences. This finding is consistent with the observations in other plant species, exposed to high Zn(II) concentrations (17, 51). ROS overproduction disrupts the integrity of chloroplast membranes and impairs photosynthetic performance (50), which is consistent with the negative correlation observed between shoot MDA content and photosynthetic pigment levels in our experiment. Contrarily, root MDA levels suggest the activation of antioxidant defense mechanisms, indicating the ability of the root system to mitigate ROS damage (27).

The accumulation of organic osmolytes, including total soluble proteins and proline, serves as crucial indicator of stress adaptation in plants. Shoots soluble protein content of *S. arundinaceus* increased with higher Zn(II) doses, while the opposite was observed in the roots. Similar findings were reported in *T. aestivum*, where HM stress led to a significant increase in shoot-soluble protein content compared to roots (35). This could be attributed to the synthesis of stress proteins or chelators, such as glutathione, phytochelatins, metallothioneins, proline or histidine, which aid in stress tolerance and HM detoxification through compartmentalization in vacuoles (19). Reduction in protein content under Zn(II) stress has also been attributed to the increased activity of proteases or catabolic enzymes induced by HM stress (28). Additionally, in our experiment, a significant increase in proline content was observed in shoots and roots at concentrations of 1500 μM and higher.

Similarly, a higher increase in proline content in the shoots of *Solanum lycopersicum* compared to the roots under Zn(II) stress was reported (4). Proline plays a significant role in osmoregulation, osmoprotection and ROS detoxification to maintain cellular homeostasis (31, 47). Additionally, it acts as a chemical chaperone and a biomembrane protector against oxidative damage, thereby stabilizing protein structure (36). Thus, proline accumulation serves as a strategy for plants to defend against oxidative stress (40). However, the positive correlation observed between shoot MDA and proline contents in *S. arundinaceus* suggests that proline increase may not fully compensate for oxidative stress. Furthermore, findings indicated that the extent of proline accumulation and its effectiveness as an osmotic adjuster are species/cultivar specific and depend on the severity and duration of the stress (34). Biomarkers have emerged as valuable tools for environmental analysis and phytoremediation programs, complementing traditional soil chemical analysis (28). Proline content demonstrated promising characteristics as a potential biomarker for Zn(II) stress in *S. arundinaceus,* as it exhibited a strong correlation with Zn(II) bioaccumulation. Also, proline determination is a cost-effective, simple and non-destructive method that can be employed at different stages of the analysis process. However, proline levels can also be influenced by other types of abiotic stresses, such as salinity and drought, resulting in varying responses depending on the plant species (20).

Conclusion

High Zn(II) concentrations affected growth, biochemical and morpho-physiological parameters of *S. arundinaceus* (principally the dry weight, photosynthetic pigments, soluble proteins, MDA and proline content). However, this species exhibited a remarkable ability to bioaccumulate high levels of Zn(II) (3432 mg kg^{-1} in shoots), surpassing phytotoxic thresholds (100-400 mg kg^{-1}) by approximately 9 times and activating stress tolerance mechanisms such as the accumulation of proline and proteins, which could act as ROS inhibitors and HM chelators. Morphological adaptations, such as smaller stomata, played

a role in maintaining a stable water content. *S. arundinaceus* performed better under 1000 and 1500 µM Zn(II), demonstrating high biomass production and Zn(II) bioaccumulation. Proline holds potential as a possible biomarker for monitoring the status of *S. arundinaceus* in response to Zn(II) stress. However, further studies are necessary to determine if similar responses occur with other HMs in the same species.

References

1. Albornoz, C. B.; Larsen, K.; Landa, R.; Quiroga, M. A.; Najle, R.; Marcovecchio, J. 2016. Lead and zinc determinations in *Festuca arundinacea* and *Cynodon dactylon* collected from contaminated soils in Tandil (Buenos Aires province, Argentina). Environ Earth Sci. 75(9): 1-8. https://doi.org/10.1007/s12665-016-5513-9
2. Alcalá Jáuregui, J. A.; Rodríguez Ortiz, J. C.; Filippini, M. F.; Martínez Carretero, E.; Hernández Montoya, A.; Rojas Velázquez, Á. N.; Méndez Cortés, H.; Beltrán Morales, F. 2022. Metallic elements in foliar material and fruits of three tree species as bioindicators. Revista de la Facultad de Ciencias Agrarias. Universidad Nacional de Cuyo. Mendoza. Argentina. 54(2): 61-72. DOI: https://doi.org/10.48162/rev.39.083
3. Anjum, N. A.; Singh, H. P.; Khan, M. I.; Masood, A.; Per, T. S.; Negi, A.; Batish, D. R.; Khan, N. A.; Duarte, A. C.; Pereira, E.; Ahmad, I. 2015. Too much is bad-an appraisal of phytotoxicity of elevated plant-beneficial heavy metal ions. Environ Sci Pollut Res. 22(5): 3361-3382. https://doi.org/10.1007/s11356-014-3849-9
4. Badiaa, O.; Yssaad, H. A. R.; Topcuoglu, B. 2020. Effect of heavy metals (Copper and Zinc) on proline, polyphenols and flavonoids content of Tomato (Lycopersicon esculentum Mill.). Plant Arch. 20: 2125-2137.
5. Bates, L. S.; Waldren, R. P.; Teare, I. D. 1973. Rapid determination of free proline for water-stress studies. Plant Soil. 39(1): 205-207. https://doi.org/10.1007/bf00018060
6. Bazihizina, N.; Redwan, M.; Taiti, C.; Giordano, C.; Monetti, E.; Masi, E.; Azzarello, E.; Mancuso, S. 2015. Root based responses account for *Psidium guajava* survival at high nickel concentration. J Plant Physiol. 174: 137-146. https://doi.org/10.1016/j.jplph.2014.10.011
7. Bilos, C.; Colombo, J. C.; Skorupka, C. N.; Presa, M. R. 2001. Sources, distribution and variability of airborne trace metals in La Plata City area, Argentina. Environ Pollut. 111(1): 149-158. https://doi.org/10.1016/S0269-7491(99)00328-0
8. Bonfranceschi, B. A.; Flocco, C. G.; Donati, E. R. 2009. Study of the heavy metal phytoextraction capacity of two forage species growing in a hydroponic environment. J Hazard Mater. 165(1-3): 366-371. https://doi.org/10.1016/j.jhazmat.2008.10.024
9. Bradford, M. M. 1976. A rapid and sensitive method for the quantitation of microgram quantities of protein utilizing the principle of protein-dye binding. Anal Biochem. 72(1-2): 248-254. https://doi.org/10.1016/0003-2697(76)90527-3
10. Briffa, J.; Sinagra, E.; Blundell, R. 2020. Heavy metal pollution in the environment and their toxicological effects on humans. Heliyon. 6(9): e04691. https://doi.org/10.1016/j.heliyon.2020.e04691
11. Brutti, L. N.; Beltran, M. J.; García de Salamone, I. 2018. Biorremediación de los recursos naturales. Ediciones INTA. Argentina.
12. Cao, A.; Cappai, G.; Carucci, A.; Muntoni, A. 2004. Selection of plants for zinc and lead phytoremediation. J Environ Sci Health. 39(4): 1011-1024. https://doi: 10.1081/ESE120028410
13. Chaparro, M. A.; Gogorza, C. S.; Chaparro, M. A.; Irurzun, M. A.; Sinito, A. M. 2006. Review of magnetism and heavy metal pollution studies of various environments in Argentina. Earth Planets Space. 58(10): 1411-1422. https://doi.org/10.1186/BF03352637
14. D'Ambrogio de Argüeso, A. 1986. Manual of techniques in plant histology. Hemisferio Sur. Buenos Aires.
15. de Strittmatter, C. D. 1973. New diaphanization technique. Bol Soc Argent Bot. 15: 126-129.
16. Di Rienzo, J. A.; Casanoves, F.; Balzarini, M. G.; González, L.; Tablada, M.; Robledo, C.W. InfoStat Versión 2020. Grupo InfoStat, FCA; Universidad Nacional de Córdoba, Argentina. http://www.infostat.com.ar
17. Dobrikova, A.; Apostolova, E.; Hanć, A.; Yotsova, E.; Borisova, P.; Sperdouli, I.; Adamakis, I. S.; Moustakas, M. 2021. Tolerance mechanisms of the aromatic and medicinal plant *Salvia sclarea* L. to excess zinc. Plants 10(2):194. https://doi.org/10.3390/plants10020194
18. Dong, Q.; Fei, L.; Wang, C.; Hu, S.; Wang, Z. 2019. Cadmium excretion via leaf hydathodes in tall fescue and its phytoremediation potential. Environ Pollut. 252: 1406-1411. https://doi.org/10.1016/j.envpol.2019.06.079
19. Emamverdian, A.; Ding, Y.; Mokhberdoran, F.; Xie, Y.; 2015. Heavy metal stress and some mechanisms of plant defense response. Sci World J. 2015: 1-18. https://doi.org/10.1155/2015/756120
20. Ghosh, U. K.; Islam, M. N.; Siddiqui, M. N.; Cao, X.; Khan, M. A. R. 2022. Proline, a multifaceted signalling molecule in plant responses to abiotic stress: understanding the physiological mechanisms. Plant Biol (Stuttg). 24(2): 227-239. https://doi.org/10.1111/plb.13363

21. Giuffré, L.; Romaniuk, R. I.; Marbán, L.; Ríos, R. P.; Torres, T. G. 2012. Public health and heavy metals in urban and periurban horticulture. Emir J Food Agric. 24(2): 148-154.
22. Gonzalez, M. A.; Ruscitti, M. F.; Plaza Cazón, J. D. C.; Arango, M. C. 2021. Bioaccumulation and physiological responses of *Festuca arundinacea* (Poaceae) to Zn(II) excess. Agronomía y Ambiente. 41(1): 13-21.
23. Hasanuzzaman, M.; Nahar, K.; Fujita, M. 2018. Plants under metal and metalloid stress: Responses, tolerance and remediation. Springer, Singapore.
24. Heath, R. L.; Packer, L. 1968. Photoperoxidation in isolated chloroplasts. Arch Biochem Biophys. 125(3): 850-857. https://doi.org/10.1016/0003-9861(68)90523-7
25. Hoagland, D. R.; Arnon, D. I. 1950. The water-culture method for growing plants without soil. Circular. California agricultural experiment station. 347(2).
26. Htwe, T.; Chotikarn, P.; Duangpan, S.; Onthong, J.; Buapet, P.; Sinutok, S. 2022. Integrated biomarker responses of rice associated with grain yield in copper-contaminated soil. Environ Sci Pollut Res. 29(6): 8947-8956. https://doi.org/10.1007/s11356-021-16314-y
27. Jan, S.; Parray, J. A. 2016. Approaches to heavy metal tolerance in plants. Springer. Singapore.
28. Kaur, H.; Garg, N. 2021. Zinc toxicity in plants: A review. Planta. 253(6): 129. https://doi.org/10.1007/s00425-021-03642-z
29. Khan, M. I. R.; Jahan, B.; Alajmi, M. F.; Rehman, M. T.; Khan, N. A. 2019. Exogenously-sourced ethylene modulates defense mechanisms and promotes tolerance to zinc stress in mustard (*Brassica juncea* L.). Plants. 8(12): 540. https://doi.org/10.3390/plants8120540
30. Kouhi, S. M.; Lahouti, M.; Ganjeali, A.; Entezari, M. H. 2016. Anatomical and ultrastructural responses of *Brassica napus* after long-termexposure to excess zinc. Turk J Biol. 40: 652-660. https://doi.org/10.3906/biy-1411-13
31. Li, X.; Yang, Y.; Jia, L.; Chen, H.; Wei, X. 2013. Zinc-induced oxidative damage, antioxidant enzyme response and proline metabolism in roots and leaves of wheat plants. Ecotoxicol Environ Saf. 89: 150-157. https://doi.org/10.1016/j.ecoenv.2012.11.025
32. López, I.; Rotger, D. V. 2020. Expansión urbana, humedales y evolución en los usos del suelo en el Gran La Plata. Biología Acuática. (35): 017. https://doi.org/10.24215/16684869e017
33. Majdoub, N.; el-Guendouz, S.; Rezgui, M.; Carlier, J.; Costa, C.; Kaab, L. B. B.; Miguel, M. G. 2017. Growth, photosynthetic pigments, phenolic content and biological activities of *Foeniculum vulgare* Mill., *Anethum graveolens* L. and *Pimpinella anisum* L. (Apiaceae) in response to zinc. Ind Crops Prod. 109: 627-636. https://doi.org/10.1016/j.indcrop.2017.09.012
34. Mansour, M. M. F.; Ali, E. F. 2017. Evaluation of proline functions in saline conditions. Phytochemistry. 140: 52-68. https://doi.org/10.1016/j.phytochem.2017.04.016
35. Mohammadi, A.; Mansour, S. N.; Najafi, M. L.; Toolabi, A.; Abdolahnejad, A.; Faraji, M.; Miri, M. 2022. Probabilistic risk assessment of soil contamination related to agricultural and industrial activities. Environ Res. 203: 111837. https://doi.org/10.1016/j.envres.2021.111837
36. Mohsenzadeh, S.; Moosavian, S. S. 2017. Zinc sulphate and nano-zinc oxide effects on some physiological parameters of *Rosmarinus officinalis*. Am J Plant Sci. 8(11): 2635-2649. https://doi.org/10.4236/ajps.2017.811178
37. Mukhopadhyay, M.; Mondal, T. K. 2015. Effect of Zinc and Boron on growth and water relations of *Camellia sinensis* (L.) O. Kuntze cv. T-78. Natl Acad Sci Lett. 38(3): 283-286. https://doi:10.1007/s40009-015-0381-5
38. Patra, D. K.; Acharya, S.; Pradhan, C.; Patra, H. K. 2021. Poaceae plants as potential phytoremediators of heavy metals and eco-restoration in contaminated mining sites. Environ Technol Innov. 21: 101293. https://doi.org/10.1016/j.eti.2020.101293
39. Peng, H.; Liang, K.; Luo, H.; Huang, H.; Luo, S.; Zhang, A.; Xu, H.; Xu, F. 2021. A bacillus and Lysinibacillus Sp. bio-augmented *Festuca arundinacea* phytoremediation system for the rapid decontamination of chromium influenced soil. Chemosphere. 283: 131186. https://doi.org/10.1016/j.chemosphere.2021.131186
40. Reddy, S. H.; Al-kalbani, H.; Al-Qalhati, S.; Al-Kahtani, A. A.; Al Hoqani, U.; Al Azmi, S. N.; Kumar, A.; Kumar, S.; Settaluri; V. S. 2024. Proline and other physiological changes as an indicator of abiotic stress caused by heavy metal contamination. Journal of King Saud University Science. 103313. https://doi.org/10.1016/j.jksus.2024.103313
41. Reyzábal, L.; Andrade, L.; Marcet, P.; Montero, M. J. 2000. Effect of long-term cultivation on zinc and copper contents in soils from the Bahía Blanca horticultural belt (Argentina). Commun Soil Sci Plan. 31(9-10): 1155-1167. https://doi.org/10.1080/00103620009370504
42. Saxena, G.; Kumar, V.; Shah, M. P.; 2020. Bioremediation for environmental sustainability: Toxicity, mechanisms of contaminants degradation, detoxification and challenges. Elsevier. Amsterdam.
43. Seethepalli, A.; York, L. M. 2020. RhizoVision Explorer-Interactive software for generalized root image analysis designed for everyone (Version 2.0.3). Zenodo. http://doi.org/10.5281/zenodo.4095629
44. Seethepalli, A.; Dhakal, K.; Griffiths, M.; Guo, H.; Freschet, G. T.; York, L. M. 2021. RhizoVision Explorer: Open-source software for root image analysis and measurement standardization. AoB PLANTS. 13(6): plab056. https://doi.org/10.1093/aobpla/plab056

45. Soto, M. B.; de las Mercedes Echeverría, M.; Lúquez, J.; San Martino, S.; Assuero, S. G.; Petigrosso, L. R. 2022. Tolerancia a la salinidad de festuca alta, naturalizada y comercial, libre e infectada con endófitos durante la germinación. Revista de la Facultad de Agronomía. 121(1): 084. https://doi.org/10.24215/16699513e084
46. Sturikova, H.; Krystofova, O.; Huska, D.; Adam, V. 2018. Zinc, zinc nanoparticles and plants. J Hazard Mater. 349: 101-110.
47. Subba, P.; Mukhopadhyay, M.; Mahato, S. K.; Bhutia, K. D.; Mondal, T. K.; Ghosh, S. K. 2014. Zinc stress induces physiological, ultra-structural and biochemical changes in mandarin orange (*Citrus reticulata* Blanco) seedlings. Physiol Mol Biol Plants. 20(4): 461-473. https://doi.org/10.1007/s12298-014-0254-2
48. Tablang, J. O.; Temanel, F. B.; Campos, R. P. C.; Ramos, H. C. 2021. Bioaccumulation of lead by pepper elder (*Peperomia pellucida* (L.) Kunth) in a lead-contaminated hydroponic system. Environ Nat Resour J. 19(4): 282-291. https://doi.org/10.32526/ennrj/19/2021010
49. Villalobos, E.; Umaña, C.; Sterling, F. 1990. Determinación del contenido relativo de agua en progenies de palma aceitera (*Elaeis guineensis*), durante la época seca en Quepos, Costa Rica. Agronomía Costarricense. 14: 73-8.
50. Waszczak, C.; Carmody, M.; Kangasjärvi, J. 2018. Reactive oxygen species in plant signaling. Annu Rev Plant Biol. 69: 209-236. https://doi.org/10.1146/annurev-arplant-042817-040322
51. Wei, C.; Jiao, Q.; Agathokleous, E.; Liu, H.; Li, G.; Zhang, J.; Fahad, S.; Jiang, Y. 2022. Hormetic effects of zinc on growth and antioxidant defense system of wheat plants. Sci Total Environ. 807: 150992. https://doi.org/10.1016/j.scitotenv.2021.150992
52. Wellburn, A. R. 1994. The spectral determination of chlorophylls a and b, as well as total carotenoids, using various solvents with spectrophotometers of different resolution. J Plant Physiol. 144(3): 307-313. https://doi.org/10.1016/s0176-1617(11)81192-2
53. Yuan, F.; Leng, B.; Wang, B. 2016. Progress in studying salt secretion from the salt glands in recretohalophytes: how do plants secrete salt? Front Plant Sci. 7: 977. https://doi.org/10.3389/fpls.2016.00977
54. Zamani, N.; Sabzalian, M. R.; Khoshgoftarmanesh, A.; Afyuni, M. 2015. Neotyphodium Endophyte changes Phytoextraction of zinc in *Festuca arundinacea* and *Lolium perenne*. Int J Phytoremediation. 17(5): 456-463. https://doi.org/10.1080/15226514.2014.922919
55. Zamora-Ledezma, C.; Negrete-Bolagay, D.; Figueroa, F.; Zamora-Ledezma, E.; Ni, M.; Alexis, F.; Guerrero, V. H. 2021. Heavy metal water pollution: A fresh look about hazards, novel and conventional remediation methods. Environ Technol Innov. 22: 101504. https://doi.org/10.1016/j.eti.2021.101504

Acknowledgments

The authors would like to thank Laura Wahnan (INFIVE-CONICET) and Cecilia Bernardelli (CINDEFI-CONICET) for technical assistance. This study was financially supported by Agencia Nacional de Promoción Científica y Tecnológica of Argentina (PICT-2016-2535), Universidad Nacional de La Plata (UNLP) (A316) and Universidad Nacional del Noroeste de la Provincia de Buenos Aires (UNNOBA) (0597/2019).